TOPICAL REVIEW — 8th IUPAP International Conference on Biological Physics

Development of mean-field electrical double layer theory*

Yike Huang(黄一珂), Xiaohong Liu(刘晓红), Shu Li(李姝), and Tianying Yan(言天英)†

School of Materials Science and Engineering, National Institute for Advanced Materials, Collaborative Innovation Center of Chemical Science and Engineering (Tianjin), Nankai University, Tianjin 300071, *China*

(Received 18 May 2015; revised manuscript received 20 July 2015; published online 8 December 2015)

In order to understand the electric interfacial behavior, mean field based electric double layer (EDL) theory has been continuously developed over the past 150 years. In this article, we briefly review the development of the EDL model, from the dimensionless Gouy–Chapman model to the symmetric Bikerman–Freise model, and finally toward size-asymmetric mean field theory models. We provide the general derivations within the framework of Helmholtz free energy of the lattice–gas model, and it can be seen that the above-mentioned models are consistent in the sense that the interconversion among them can be achieved by reducing the basic assumptions.

Keywords: electric double layer, mean field theory, differential capacitance, supercapacitor

PACS: 68.08.–p, 68.08.De, 73.30.+y, 82.47.Uv **DOI:** 10.1088/1674-1056/25/1/016801

1. Electric double layer (EDL)

Electric double layer exists widely in biology and materials. Nowadays, the demand on the higher energy density of the supercapacitor has become stronger, due to its high power density. Graphene with a high surface area as well as the ionic liquid (IL) with many unique properties, make them highly desirable. Thus, a theoretical understanding on the capacitance behavior on such newly developed materials is greatly needed. Over the past 100 years, a mean-field theory (MFT), such as the Gouy–Chapman EDL model, is referred to frequently. Later, the re-discovery and new development of the mean field based EDL theory also attracted a great deal of attention. In this review, we briefly overview the development of mean field based EDL theory.

The first EDL model was proposed by Helmholtz,[1,2]

$$C_{\mathrm{H}} = \frac{\varepsilon\varepsilon_0}{d}, \tag{1}$$

in which ε is relative dielectric constant, ε_0 is permittivity of free space, and d is the width between the two oppositely charged parallel plates. Equation (1) can be found in fundamental physics textbooks for the specific capacitance C_{H} of parallel plate capacitor, which implies that the capacitance would be much enhanced with higher ε and shorter distance d between the two plates.

Equation (1) provides a vivid picture for the electrochemical capacitor or the so-called supercapacitor. Considering the interface between a charged electrode and ionic electrolyte, as depicted in Fig. 1, the counterions will accumulate on the electrode due to the electrostatic interactions. Such arrangement may be analogous to the parallel plate capacitor, with the other plate forming by the counter ion layer. A distinct feature of such a capacitor is that the distance between the two "plates" is much shortened. Theoretically, the distance is often attributed to the radius of the ions on the nanometer scale. Due to such short distance d, the capacitance C_{H} by Eq. (1) is much enhanced, and a capacitor formed by such EDL is the so-called electrochemical capacitor or supercapacitor.

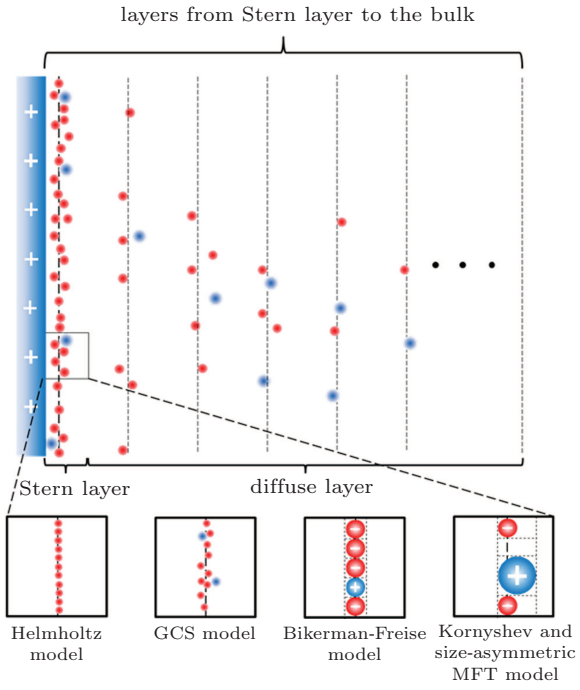


Fig. 1. Scheme of electric double layer (EDL). The single charged ion layer adjacent to the electrode forms the compact layer or Stern layer, while the outer layer forms the diffuse layer. The series of the two layers is called the Gouy–Chapman–Stern (GCS) EDL model.

*Project supported by the National Natural Science Foundation of China (Grant Nos. 21421001, 21373118, and 21203100), the Natural Science Foundation of Tianjin, China (Grant No. 13JCQNJC06700), the MOE Innovation Team of China (Grant No. IRT13022), and NFFTBS (Grant No. J1103306).

†Corresponding author. E-mail: tyan@nankai.edu.cn

© 2016 Chinese Physical Society and IOP Publishing Ltd

2. Gouy–Chapman–Stern (GCS) model

Since such a simple and clear picture is given by Eq. (1), it is frequently adopted experimentally for the supercapacitance behavior.[3] It is also notable that Eq. (1) is a highly simplified model, nevertheless in a real electrolyte solution, the EDL structure is much more complicated. Clearly, the distribution of the counterions is not a single charged layer close to the electrode surface. A more realistic picture is the diffuse layer as in Fig. 1, as proposed by Gouy[4] and Chapman.[5]

In the Gouy–Chapman model, the number density of monovalence ion in the electrolyte solution is given by the Boltzmann distribution

$$c_{\pm} = c_{\infty} \mathrm{e}^{\mp e\phi/kT}, \tag{2}$$

in which c_+ and c_- are the density of the cation and anion, respectively, c_{∞} is the equilibrium bulk density of individual ions far from the electrode at $x = 0$, e is the elementary electron charge, ϕ is the electrostatic potential, k is Boltzmann constant, and T is the temperature. The Boltzmann distribution in Eq. (2) is a mean field approximation to the ionic density, and the charge density ρ in the diffuse layer is given by

$$\rho = e(c_+ - c_-) = -2ec_{\infty} \sinh\left(\frac{e\phi}{kT}\right). \tag{3}$$

Equation (3) gives charge density of 1:1 electrolyte system, for which an analytical expression of differential capacitance is available. Appling Poisson equation, i.e.,

$$\frac{\mathrm{d}^2\phi}{\mathrm{d}x^2} = -\frac{\rho}{\varepsilon\varepsilon_0}, \tag{4}$$

the differential capacitance C_d is given by

$$C_\mathrm{d} = \frac{\varepsilon\varepsilon_0}{\lambda_\mathrm{D}} \cosh\left(\frac{e\phi_0}{2kT}\right), \tag{5}$$

in which ϕ_0 is the electrode potential, and λ_D is the Debye length, i.e.,

$$\lambda_\mathrm{D} = \sqrt{\frac{\varepsilon\varepsilon_0 kT}{2e^2 c_{\infty}}}. \tag{6}$$

This Gouy–Chapman model in Eq. (5) differs from the Helmholtz model of Eq. (1) in its extra dependence on ϕ_0. From the electrochemical perspective, C_d in Eq. (5) is the natural response of the electrode potential dependent EDL at different ϕ_0, which alters EDL structures and results in different C_d. However, the hyperbolic cosine function in Eq. (5) implies that C_d increases with ϕ_0, and this never happens in reality. In order to remedy this, Stern[6] proposed the series of Eqs. (1) and (5), so that the capacitance is given by

$$\frac{1}{C} = \frac{1}{C_\mathrm{H}} + \frac{1}{C_\mathrm{GC}}, \tag{7}$$

in which C_H and C_GC are given by Eqs. (1) and (5), respectively.

Equation (7) is well known as the Gouy–Chapman–Stern (GCS) model. Since its scientific intuition form, it has been widely accepted and bears the standard definition of an electric double layer, as shown in Fig. 1.[1] Besides, the success of the GCS model has been demonstrated in tremendous works.[6,7]

3. Bikerman model

The Gouy–Chapman model implies that C_d increases with ϕ_0, and this is indeed applicable in the case at low ϕ_0 for dilute electrolyte solutions. However, experiments on strong electrolytes and ILs often show the opposite trends. Instead of the parabola-shaped C_d at low ϕ_0, it may be bell-shaped.[8] Also, at high ϕ_0, C_d generally shows a decreasing wing, which cannot be captured by the GCS model either. For the latter, the high ϕ_0 region is constant, with the C_d fixed by the Helmholtz model.

One of the important reasons for the failure of the GCS model, especially at the high ϕ_0 region, is attributed to the ionic size effect. The infinite high C_d at high ϕ_0 in the Gouy–Chapman model is caused by the underneath assumption of the dimensionless ions that are capable of accumulating at the EDL toward infinite density in order to screen a high ϕ_0. In reality, it is definitely not the case, because the size of ions prevents its high density, even with the closest packing.

In the mean-field theory, the ionic size effect may be casted by a two dimensional lattice-gas model, as shown in Fig. 2. Note that figure 2 may be any infinite thin layer parallel to the electrode surface, and the ion/solvent distribution varies from layer to layer in the EDL, while it is constant in the bulk region at infinite distance toward the electrode surface.

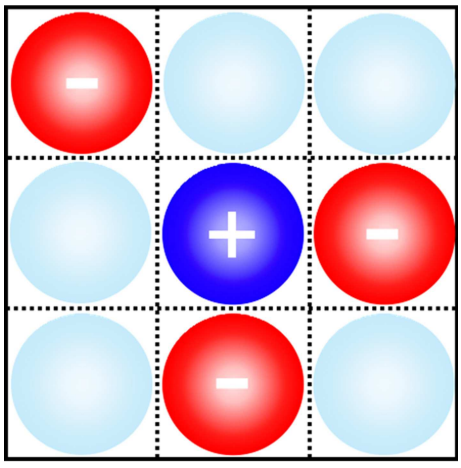


Fig. 2. A two-dimensional representation of the mean field lattice-gas model, in which blue hard spheres represent cations, red hard spheres represent anions, and iceblue hard spheres represent the solvent molecules or empty space for pure ionic electrolyte, such as ILs.

By taking into account ion sizes, Bikerman proposed an EDL model in 1942.[9] Bikerman's model may be easily un-

derstood with the lattice-gas scheme in Fig. 2. Note that the volume is constant for such a system, so that the derivation starts with the Helmholtz free energy, F, of the lattice-gas model,

$$F = e\phi(N_+ - N_-) - kT\ln\Omega, \tag{8}$$

in which N_+ and N_- are the number of cations and anions in the lattice, and Ω is the partition function given by

$$\Omega = \frac{N!}{N_+!N_-!N_s!}, \tag{9}$$

in which N_s and N are the number of solvent molecules and the total number of ions/molecules in the lattice.

The underlying assumption of the Bikerman model is the constant total number, i.e.,

$$N = N_+ + N_- + N_s. \tag{10}$$

The above constraint implies $\partial N_s/\partial N_\pm = -1$. Thus, by taking the chemical potential of each kind of ions, i.e., $\mu_\pm = \partial F/\partial N_\pm$ and using Sterling approximation $\ln N_\pm! = N_\pm \ln N_\pm - N_\pm$, we have

$$\mu_\pm = e\phi + kT\ln\frac{N_\pm}{N_s}. \tag{11}$$

Remembering the fact that the chemical potential of each component is equal everywhere for an equilibrium system, i.e., $\mu_\pm = \mu_\infty$, and $\phi_\infty = 0$, $N_{+,\infty} = N_{-,\infty} = N_\infty$ in the bulk lattice, the numbers of ions in different layers are given by

$$N_\pm = N_\infty \mathrm{e}^{\mp e\phi/kT}\frac{N - N_+ - N_-}{N - 2N_\infty}. \tag{12}$$

Note that equation (12) is correct for any sizes of ions and solvent molecules for the lattice–gas model in Fig. 2, with constant number constraint in Eq. (10). In the following derivation, Bikerman took into account the constant volume of each layer, i.e.,

$$V = V_+ + V_- + V_s = N_+v_+ + N_-v_- + N_sv_s, \tag{13}$$

in which v_+, v_-, and v_s are the ionic/molecular volumes of cations, anions, and solvent molecules, respectively. Assuming $v_+ = v_- = v_s$, then Eqs. (10) and (13) are equivalent, and the ionic density distribution may be written as

$$c_\pm = c_\infty \mathrm{e}^{\mp e\phi/kT}\frac{1 - c_+v_+ - c_-v_-}{1 - c_\infty(v_+ + v_-)}, \tag{14}$$

in which $c_\pm = N_\pm/V$ and $c_\infty = N_\infty/V$ are the densities of ions in EDL and in bulk, respectively.

Equation (14) is re-derived in the lattice-gas scheme, for the reason that Bikerman presented it with no explicit derivation.[9] Note that the Gouy–Chapman model can also be derived in a similar manner, with an additional assumption of $N_s \to \infty$, though the original derivations were performed in terms of osmotic or hydrostatic pressure.[4,5] Thus, the Gouy–Chapman model is often referred to as an infinite dilute model.

Comparing with the Boltzmann distribution in Eq. (3), we can see that the modified Boltzmann distribution in Eq. (14) is the consequence of ionic sizes. Thus, instead of infinite $c_\pm$, the density at infinite ϕ_0 in Eq. (2), which is surpassed in Eq. (14) by the fractional term. Thus, C_d decreases at high ϕ_0 with a square-root decay wing.[10] Bikerman also pioneered on taking into account the polarizable effects manifested in the dipole moment of the coordinated solvents,[9] which is beyond this short review.

4. Freise model

From the previous section, it can be seen that the ionic density distribution of the Bikerman model is derived for the ions/solvent molecules of equal sizes. Though equation (14) does not prevent its further applications on the ions/solvent molecules of different sizes, the inherent inconsistence is imposed by the constant number constrain of EDL. The reason is that the constant number constraint in Eq. (10) is not consistent with the constant volume constraint in Eq. (13), except all the ions and solvent molecules have equal sizes. For different sizes, a constant volume constraint means the numbers vary at different EDL. Thus, as pointed out by Freise,[11] equation (13) is more reasonable for the EDL model of asymmetric ions and solvent molecules.

The Freise model can also be understood within the framework of the lattice–gas mean field model in Fig. 2, with the constant volume constraint by Eq. (13), which implies that $\partial N_s/\partial N_\pm = -v_\pm/v_s$. The derivation follows the Bikerman model in Section 3, and the numbers of ions in different layers are given by

$$N_\pm = N_\infty \mathrm{e}^{\mp e\phi/kT}\left(\frac{N_s}{N - 2N_\infty}\right)^{v_\pm/v_s}. \tag{15}$$

The above expression includes the ionic size effect as comparing to Eq. (12). For $v_+ = v_- = v_s$, equation (15) reduces to Eq. (12).[11] It is notable that N_s in Eq. (15) should not be obtained by Eq. (10) for ions/solvent molecules of different sizes, but by Eq. (13). However, it appears that the Freise model takes Eq. (10) for N_s, and the ionic density distributions are written as

$$c_\pm = c_\infty \mathrm{e}^{\mp e\phi/kT}\left(\frac{1 - \gamma_+ - \gamma_-}{1 - 2\gamma_\infty}\right)^{v_\pm/v_s}, \tag{16}$$

in which $\gamma_\pm = c_\pm/(c_+ + c_- + c_s)$, γ_+, and γ_- is the molar fraction of cation and anion, respectively, and γ_∞ denotes the molar fraction of ions in the bulk where $\gamma_{+,\infty} = \gamma_{-,\infty} = \gamma_\infty$.

As discussed above, equation (16) is derived from Eq. (15) with constant number constraint by Eq. (10), thus it is

not consistent with the constant volume constraint either. It is of interest to note that equation (16) was rigorously derived by Freise[11] in terms of osmotic pressure, similar to Gouy[4] and Chapman,[5] instead of the chemical potential as in Section 3. However, it is inappropriate to apply the osmotic pressure to the solvents, and that may cause the inconsistence between Eqs. (15) and (16). Since the Bikerman model and the Freise model are very similar, they are called the Bikerman–Freise model.[7]

Nevertheless, for $v_+ = v_- = v_s = v$, equations (16) and (14) become equivalent as $\gamma_\pm = c_\pm v$ in this case, and both are correct for the ions/molecules of equal sizes. Indeed, this is a big step on the improvement of the Gouy–Chapman model for the dimensionless ions. For the equal ionic/molecular sizes, the ionic distribution may be written as[7]

$$c_\pm = c_\infty \mathrm{e}^{-ze\phi/kT} \frac{1}{1+4c_\infty v \sinh^2\left(\dfrac{e\phi}{2kT}\right)}. \tag{17}$$

Thus, the charge density in EDL according to Eq. (2) is[7,12,13]

$$\rho = -2ec_\infty \frac{\sinh\left(\dfrac{e\phi}{kT}\right)}{1+4c_\infty v \sinh^2\left(\dfrac{e\phi}{2kT}\right)}. \tag{18}$$

Solving the Poisson function in Eq. (4), and Freise further derived the analytical expression of C_d, i.e.,[7,8,10–12,14]

$$C_\mathrm{d} = \mathrm{sgn}(\phi_0)\frac{\varepsilon\varepsilon_0}{\lambda_\mathrm{D}} \frac{\sinh\left(\dfrac{e\phi_0}{kT}\right)}{1+4c_\infty v \sinh^2\left(\dfrac{e\phi_0}{2kT}\right)} \times \sqrt{\frac{c_\infty v}{\ln\left[1+4c_\infty v \sinh^2\left(\dfrac{e\phi_0}{2kT}\right)\right]}}, \tag{19}$$

in which sgn denotes sign function and $v_+ = v_- = v_s = v$ for ions/molecules of equal sizes. It is notable that equation (19) reduces to the Gouy–Chapman model, Eq. (5), in the $v \to 0$ limit for the dimensionless ions, using the identities

$$\ln\left[1+4c_\infty v \sinh^2\left(\frac{e\phi_0}{2kT}\right)\right] \approx 4c_\infty v \sinh^2\left(\frac{e\phi_0}{2kT}\right),$$

$$1+4c_\infty v \sinh^2\left(\frac{e\phi_0}{2kT}\right) \approx 1,$$

and

$$\sinh\left(\frac{e\phi_0}{kT}\right) = 2\sinh\left(\frac{e\phi_0}{2kT}\right)\cosh\left(\frac{e\phi_0}{2kT}\right).$$

The above expression was re-discovered many times during the following half century.[7] However, even Freise was not the first person to get Eq. (19). In fact, Stern derived a similar expression of C_d in 1924,[6] which was almost forgotten in history,[7,11] partly due to the glory of the GCS model proposed in the same milestone paper.[6]

5. Kornyshev model

The omission of the ionic size effect addressed by the Bikerman-Freise model for the following half century is reasonable, because the GCS model can often be applied on the C_d and EDL properties of dilute electrolyte reasonably well. With the development of ILs since 2000, the capacitance properties of this new kind of room temperature molten salts have caught a great deal of attention. Interestingly, it is often found that C_d curves of ILs are bell-shaped, in contrast to the traditional parabola-shaped C_d at low applied potential.[10,12,14]

In 2007, Kornyshev[10] and Kilic, Bazant, and Ajdari[12] independently published two papers on the EDL of equally sized ions. While Bazant *et al.*[12] orientated on the strong electrolyte system for the diffusion process, Kornyshev[10] specifically orientated toward ILs for the differential capacitance, C_d. Both works are based on the mean field lattice-gas model as shown in Fig. 2, and derived the analytical expression of C_d, which is essentially the same as Eq. (19) by Freise, as expected. It is of interest to note that both works were stimulated by Borukhov, Andelman, and Orland,[15] which is actually another example of the re-discovery of the Bikerman–Freise model, and it appears that Freise's work was not realized by either of these authors.

In Kornyshev's well-celebrated work,[10] the effects of ionic size on C_d of ILs are vividly described by γ_∞ defined by Freise.[11] Since ions are equally sized with the same volume $v_+ = v_- = v$, equations (10) and (13) are equivalent, so that the molar fraction of individual ion in the bulk is

$$\gamma_\infty = \frac{c_\infty}{2c_\infty + c_{\mathrm{s},\infty}} = \frac{N_\infty}{N} = c_\infty v, \tag{20}$$

in which $c_{+,\infty} = c_{-,\infty} = c_\infty$ is the ionic density in the bulk, $c_{\mathrm{s},\infty}$ is the solvent density (or empty lattice density, e.g., Fig. 2) in the bulk. N_∞ is the equilibrium number of individual ions in the bulk lattice, and $N_{+,\infty} = N_{-,\infty} = N_\infty$. Based on Eq. (20), Kornyshev further defined compressibility by

$$\gamma = 2\gamma_\infty. \tag{21}$$

Thus, in Kornyshev's derivation, the term $4c_\infty v$ in Eq. (19) is replaced by 2γ.[10]

The significance of γ may be illustrated by Fig. 2 for the bulk lattice. For $\gamma = 1$, all the lattices are completely occupied by the ions. For $\gamma \to 0$, equation (19) reduces to the Gouy–Chapman model, as discussed in Section 4. For $\gamma > 0$, then all the lattices are partially occupied by the ions. Thus, counterions cannot approach the electrode with infinite density, but instead "crowding" at the interface and may extend several EDL layers at high electrode potential. Such an effect manifests in Eq. (19) by taking the high ϕ_0 limit with

$$\sinh(e\phi_0/kT) \approx \exp(e\phi_0/kT)/2,$$

and

$$\sinh^2(e\phi_0/2kT) \approx \exp(e\phi_0/kT)/4,$$

so that[10]

$$C_{\rm d} \approx \frac{\varepsilon\varepsilon_0}{\lambda_{\rm D}}\sqrt{\frac{kT}{2\gamma e|\phi_0|}}. \tag{22}$$

The above expression of $C_{\rm d}$ for the high ϕ_0 limit was first given by Kornyshev[10] to the authors' best knowledge, though such inverse-square-root decay of $C_{\rm d}$ on the high ϕ_0 was indicated by Bikerman.[9]

By taking the low ϕ_0 limit, equation (19) may be written as[10]

$$C_{\rm d} \approx \frac{\varepsilon\varepsilon_0}{\lambda_{\rm D}}\left[1+\frac{1-3\gamma}{8}\left(\frac{e\phi_0}{kT}\right)^2\right]. \tag{23}$$

It can be clearly seen from Eq. (23) that $C_{\rm d}$ increases with ϕ_0 for $\gamma < 1/3$ at low ϕ_0 and results in an overall camel-shaped $C_{\rm d}$, while it monotonically decreases with ϕ_0 for $\gamma > 1/3$ and results in an overall bell-shaped $C_{\rm d}$. Equation (19), as well as its high ϕ_0 and low ϕ_0 behavior, has been verified by many recent experiments and simulations on the $C_{\rm d}$ of ILs.[14] Thus, Kornyshev's work in 2007,[10] though it represented another re-discovery of the Bikerman–Freise model, stimulated tremendous interest in the development of EDL theory for the pure ionic electrolytes.

It should be addressed that $C_{\rm d}$ in Eq. (19) was derived explicitly for the symmetric ions of equal sizes. For asymmetric ions with different cation and anion sizes, that is, $v_+ \neq v_-$, the lattice–gas model can be represented by Fig. 3, in which an obvious fact is that the compressibilities of cations and anions are different. Thus, for asymmetric ions of different compressibilities, $\gamma_+ \neq \gamma_-$, Kornyshev proposed the semi-empirical u_0-dependent γ as[10]

$$\gamma(u_0) = \gamma_- + \frac{\gamma_+ - \gamma_-}{1+{\rm e}^{u_0}}, \tag{24}$$

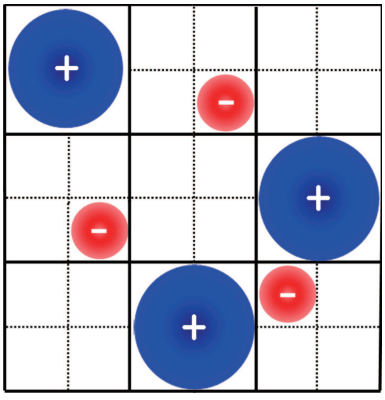


Fig. 3. A two-dimensional representation of the mean field lattice–gas model for ILs, in which blue hard spheres represent cations, and red hard spheres represent anions. The space is divided into lattices by the solid line to accommodate cations, and then subdivided by dotted line to accommodate anions, in order to take into account different cationic and anionic sizes.

where u_0 is the dimensionless potential, and $u_0 = e\phi_0/kT$. The above semi-empirical γ, in combination with Eq. (19), represents the Kornyshev model for the $C_{\rm d}$ of asymmetric ions, and the results are reasonably good, as will be compared below.

6. Size-asymmetric mean field theory (SAMFT) model

For the lattice-gas model in Fig. 3 of asymmetric ions of volume ratio $\xi = v_-/v_+ = \gamma_-/\gamma_+$, Han *et al.* attempted to get the partition function via two steps, i.e., $\Omega = \Omega_+\Omega_-$. For the total available lattices N that are capable of accommodating cations N_+, and the left are for anions, $(N-N_+)/\xi$. Based on the above consideration, the partition function of the lattice-gas model in Fig. 3 may be written as[8]

$$\Omega = \frac{N!}{N_+!(N-N_+)!}\cdot\frac{[(N-N_+)/\xi]!}{N_-!\{[(N-N_+)/\xi]-N_-\}!}. \tag{25}$$

Following the derivation in terms of the Helmholtz free energy in Section 3, the charge density is given by[8]

$$\rho = \frac{2ec_\infty}{\gamma}\frac{{\rm e}^{-e\phi/kT} - {\rm e}^{e\phi/kT}\left(\dfrac{\xi\,{\rm e}^{e\phi/kT}+\eta}{\xi+\eta}\right)^{1/\xi-1}}{{\rm e}^{-e\phi/kT} + (\xi+\eta)\left(\dfrac{\xi\,{\rm e}^{e\phi/kT}+\eta}{\xi+\eta}\right)^{1/\xi}}, \tag{26}$$

in which $\gamma = \gamma_+$ for the compressibility of cations and $\eta = 2/\gamma - 1 - \xi$ is the porosity. It should be addressed that equation (26) is also a re-discovery of Chu's work in 2007. This equation is successfully formulated by Chu *et al.* In fact, the equation formulated by Chu *et al.* has a more widely scope of application, because it can be used on not only 1:1 ILs but also 1:z ILs.[17] Lu and Zhou also formulated size-modified MFT for asymmetric ions, and incorporated to the size-modified Poisson–Nernst–Planck (SMPNP) equation for the diffusion process in biological systems.[18]

It can be shown that as $\xi = 1$ the above equation reduces to Eq. (18), using the relations $\sinh(e\phi_0/kT) = [\exp(e\phi_0/kT) - \exp(-e\phi_0/kT)]/2$ and $\sinh^2(e\phi_0/2kT) = [\exp(e\phi_0/kT) + \exp(-e\phi_0/kT) - 2]/4$. In the $\phi \to 0$ limit, using the first order approximations, it can be shown that Eq. (26) reduces to

$$\rho \approx -\left(2+\frac{1-\xi}{\xi+\eta}\right)\frac{c_\infty e^2\phi}{kT}. \tag{27}$$

From the above approximation, it can be seen that for asymmetric ions $\xi < 1$, the EDL charge density may well exceed that of the dimensionless ion predicted by the Gouy–Chapman model in Eq. (3) or the Bikerman–Freise model in Eq. (18), which give $\rho \approx -2c_\infty e^2\phi/kT$ in the $\phi \to 0$ limit. Such an effect is amplified as $\xi \to 0$ and $\gamma \to 1$.[8]

Solving the Poisson equation (4) with charge density in Eq. (26), the analytical $C_{\rm d}$ in the SAMFT model is[8]

$$C_{\rm d} = \mathrm{sgn}(\phi_0)\frac{\varepsilon\varepsilon_0}{\lambda_{\rm D}}\frac{1}{\sqrt{2\gamma}}\frac{\mathrm{e}^{e\phi_0/kT}\left(\dfrac{\xi\,\mathrm{e}^{e\phi_0/kT}+\eta}{\xi+\eta}\right)^{1/\xi-1} - \mathrm{e}^{-e\phi_0/kT}}{\mathrm{e}^{-e\phi_0/kT}+(\xi+\eta)\left(\dfrac{\xi\,\mathrm{e}^{e\phi_0/kT}+\eta}{\xi+\eta}\right)^{1/\xi}}$$
$$\times\left(\sqrt{\ln\left[\mathrm{e}^{-e\phi_0/kT}+(\xi+\eta)\left(\frac{\xi\,\mathrm{e}^{e\phi_0/kT}+\eta}{\xi+\eta}\right)^{1/\xi}\right]+\ln\frac{\gamma}{2}}\right)^{-1}. \quad (28)$$

Though the above $C_{\rm d}$ in the SAMFT model looks complicated, it is inherent from the Gouy–Chapman and Bikerman–Freise models. As can be seen that equation (28) reduces to Eq. (19) for $\xi = 1$, which further reduces to Eq. (5) in the $\gamma \to 0$ limit. Also, the high ϕ_0 limit of Eq. (28) gives[8]

$$\begin{aligned} C_{\rm d} &\approx \frac{\varepsilon\varepsilon_0}{\lambda_{\rm D}}\sqrt{\frac{kT}{2\xi\gamma e\phi_0}}, \text{for high positive } \phi_0, \\ C_{\rm d} &\approx \frac{\varepsilon\varepsilon_0}{\lambda_{\rm D}}\sqrt{\frac{kT}{2\gamma e|\phi_0|}}, \text{for high negative } \phi_0. \end{aligned} \quad (29)$$

Remembering that $\gamma_+ = \gamma$ and $\gamma_- = \xi\gamma$, the above inverse-square-root decay is consistent with Eq. (22) for the symmetric ions of $\xi = 1$, but includes a "crowding" effect for the positive polarization branch and negative polarization branch characterized by the size of counter ions in the high ϕ_0 wing.

At low electrode potential ϕ_0, the $C_{\rm d}$ of the Gouy–Chapman theory in Eq. (5) imposes the upper limit of the Kornyshev model[10] and the Bikerman–Freise model[9,11] in Eq. (19) either with semi-empirical potential-dependent $\gamma(u_0)$ or with constant γ in Eq. (24), as shown in Fig. 4(a). On the other hand, this is not the case for Eq. (28). With decreasing γ, both Eqs. (19) and (28) approach asymptotically Eq. (5) from the upper and lower sides.

Considering asymmetric ionic liquids, the $C_{\rm d}$ at the negative branch obtained by Kornyshev using the semi-empirical Eq. (24) with Eq. (19) for $\gamma_+ = 1.0$ and $\gamma_- = 0.5$ is consistent with the Bikerman–Freise model ($\gamma = 1.0$ and $\gamma = 0.5$), while that at the positive branch agrees well with the Bikerman–Freise model for $\gamma = 1.0$. It should be mentioned that the $C_{\rm d}$ at the potential of zero charge (PZC) predicted by the SAMFT model can be higher than the Debye capacitance, with $C_{\rm d}$ in the other models equal the Debye capacitance.

The $C_{\rm d}$ curves become camel-shaped for the Kornyshev model[10] for $\gamma_+ = 0.1$ and $\gamma_- = 0.01$ and the Bikerman–Freise model[9,11] for $\gamma = 0.1$ and $\gamma = 0.01$ in Fig. 4(b). Comparing the four curves in Fig. 4(b), it can be seen that the values of $C_{\rm d}$ of the SAMFT model are closer to the results by the Bikerman-Freise model than the Kornyshev model with semi-empirical potential-dependent $\gamma(u_0)$ or with constant γ. Meanwhile, the Bikerman–Freise model, Kornyshev model and SAMFT model successfully predict the inverse-square-root law resulted from "crowding" of counter ions. Such a crowding phenomenon of counterions, as shown in the illustration of Fig. 4, may increase the thickness of the compact layer or Stern layer and decrease the capacitance.

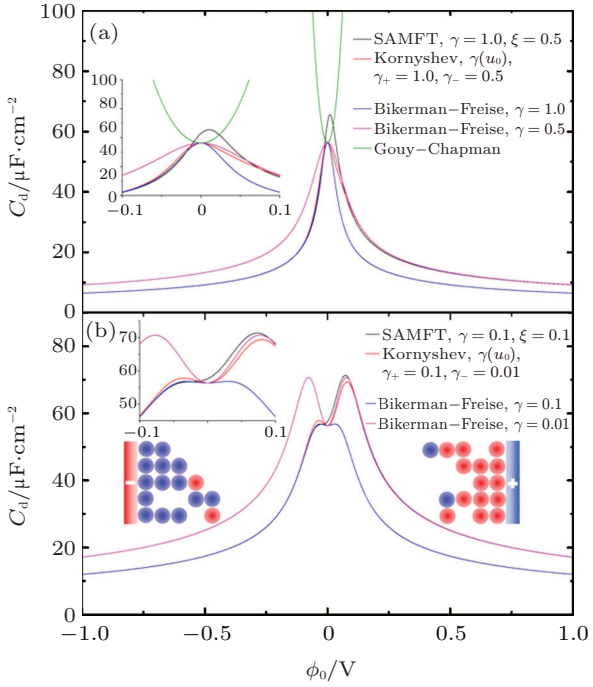


Fig. 4. $C_{\rm d}$ at different levels of theory. (a) $C_{\rm d}$ by Eq. (28) with $\gamma = 1.0$, $\xi = 0.5$ (black), Eq. (19) with semi-empirical $\gamma(\phi_0)$ in Eq. (24) for $\gamma_+ = \gamma = 1.0$ and $\gamma_- = \xi\gamma = 0.5$ (red), Eq. (19) with $\gamma = 1.0$ (blue) and $\gamma = 0.5$ (pink), with Eq. (5) (green). (b) $C_{\rm d}$ by Eq. (28) with $\gamma = 0.1$, $\xi = 0.1$ (black), Eq. (19) with semi-empirical $\gamma(\phi_0)$ in Eq. (24) for $\gamma_+ = \gamma = 0.1$ and $\gamma_- = \xi\gamma = 0.01$ (red), Eq. (19) with $\gamma = 0.1$ (blue) and $\gamma = 0.01$ (pink). Insets in (a) and (b) are $C_{\rm d}$ at different levels of theory between potentials of -0.1 to 0.1 V.

7. Summary

In this article, we briefly reviewed the development of the mean field based EDL theory from the Helmholtz model to the SAMFT model. Though the effects of the ionic size on the EDL and $C_{\rm d}$ was studied by the Bikerman–Freise model more than half a century ago, the re-discovery of this theory was experimentally called by the new electrolyte materials, ILs.[10] Based on these efforts, the SAMFT model further provides a $C_{\rm d}$ for asymmetric 1:1 IL in Eq. (29), which reduces to the Bikerman–Freise model, and the Gouy–Chapman model for dimensionless ions.

It should be noted that the lattice-gas models presented in Figs. 2 and 3 vary with the distance to the electrode surface and electrode potential. Furthermore, the lattice-gas model is actually two-dimensional and is inifinite thin along the electrode surface normal direction, in order to apply the continuous differentiation with a one-dimensional Poisson equation (4). As a matter of fact, this is an inherent limitation of mean field theory for the analytical expressions. This inconsistence of sized ions may be remedied by a series of a Stern layer, as has been applied by Kornyshev for the extended Bikerman–Freise model.[16]

Finally, we mentioned that the current review only focussed on mean field EDL theory. The benefit is that the analytical expressions can often be derived, and such a simple model can often help to understand the complex experimental results in a qualitative manner with a vivid picture. Of course, the mean field based EDL theory oversimplified the real situation. For example, overscreening, or charge inversion effect, caused by the correlations between cations and anions, cannot be treated by the mean field framework. For the latter, density functional theory and computer simulations that are well beyond the scope of this article, can often be applied to get more realistic results, though the analytical expressions are lost with simple pictures.

References

[1] Bard A J and Faulkner L R 1980 *Electrochemical Methods Fundamentals and Applications*, 2nd edn. (Beijing: Chemical Industry Press) pp. 379–384 (in Chinese)
[2] Helmholtz H 1853 *Ann. Phys.* **89** 211
[3] Chmiola J, Yushin G, Gogotsi Y, Portet C, Simon P and Taberna P L 2006 *Science* **313** 1760
[4] Gouy L G 1910 *J. Phys. Theor. Appl.* **9** 457
[5] Chapman D L 1913 *Philos. Mag.* **25** 475
[6] Stern O 1924 *Z. Elektrochem.* **30** 508
[7] Bazant M Z, Kilic M S, Storey B D and Ajdari A 2009 *Adv. Colloid Interface Sci.* **152** 48
[8] Han Y N, Huang S H and Yan T Y 2014 *J. Phys.: Condens. Matt.* **26** 284013
[9] Bikerman J J 1942 *Philos. Mag.* **33** 384
[10] Kornyshev A A 2007 *J. Phys. Chem. B* **111** 5545
[11] Freise 1952 *Z. Elektrochem.* **56** 822
[12] Kilic M S, Bazant M Z and Ajdari A 2007 *Phys. Rev. E* **75** 021502
[13] Kilic M S, Bazant M Z and Ajdari A 2007 *Phys. Rev. E* **75** 021503
[14] Fedorov M V and Kornyshev A A 2014 *Chem. Rev.* **114** 2978
[15] Borukhov I, Andelman D and Orland H 1997 *Phys. Rev. Lett.* **79** 435
[16] Fedorov M V and Kornyshev A A 2008 *J. Phys. Chem. B* **112** 11868
[17] Chu V B, Bai Y, Lipfert J and Doniach S 2007 *Biophys. J.* **93** 3202
[18] Lu B Z and Zhou Y C 2011 *Biophys. J.* **100** 2475